ONE-MINUTE ASSESSMENT OF PHOTOSYNTHETICALLY ACTIVE RADIATION (PAR) MODELS IN URUGUAY

José Luis Di Laccio[1], Rodrigo Alonso-Suárez[2,*], Gonzalo Abal[3]

1. Departamento de Física, CeRP del Litoral, Florencio Sánchez 396, C.P. 50000, Salto, Uruguay
2. Laboratorio de Energía Solar, Instituto de Física, Facultad de Ingeniería, Universidad de la República, Julio Herrera y Reissig 565, C.P. 11300, Montevideo Uruguay.
3. Laboratorio de Energía Solar, Departamento de Física, CENUR Litoral Norte, Universidad de la República, Av. L. Batlle Berres km 508, C.P. 5000, Salto, Uruguay.

***e-mail**: rodrigoa@fing.edu.uy

Abstract

Photosynthetically Active Radiation (PAR) is the spectral portion of global solar radiation (between 400 and 700 nm) relevant to a plant's growth processes. The PAR fraction (f_p) is the ratio at horizontal surface between the photon's flux per square meter (Q_p) and the global solar irradiance (G_h). In this work, the first assessment in Uruguay of PAR fraction empirical models is presented using 4 years of 1-minute measured data for one site representative of the Pampa Húmeda region. The chosen models have been developed for the 1-hour time scale and use the clearness index and/or the solar altitude as predictive variables. Original and locally adjusted versions of these models are evaluated and compared with the utilization of a constant value for PAR fraction (frequently used in agronomical practice). It is found that polynomial k_t models with original coefficients have acceptable performance, but they cannot be used with locally adjusted coefficients at the 1-minute timescale.

Keywords: PAR radiation, PAR fraction, empirical models, GHI.

1. Introduction

Photosynthetically Active Radiation (PAR) is the portion of solar radiation in the spectral interval 400-700 nm. This radiation is used by plants for photosynthesis and its characterization in a given region is highly relevant for plant growth rates and for an adequate planning of agricultural production. PAR radiation is measured by specialized sensors as the photon flux (in the 400-700 nm interval) per unit area and expressed as μmol/m^{2}s. On a horizontal surface, this magnitude is denoted by Q_p and it is highly correlated with the global horizontal irradiance, G_h or GHI. If a specialized sensor is not available, Q_p can be indirectly estimated from pyranometer measurements by using an infrared filter which effectively blocks solar irradiance above 700 nm. One of the problems associated with this approach is that, unless an independent UV measurement is available, all UV irradiance below 400 nm will be counted as PAR radiation. For locations for which no PAR measurements are available, Q_p can be estimated from GHI using either a constant PAR fraction or an empirical model, being the latter a lower uncertainty option.

The PAR fraction, which is the quantity of interest in this work, is the ratio $f_p = Q_p/G_h$ expressed in μmol/J. Several previous studies (see for example Tsubo and Walker, 2007) have reported mean PAR fractions between 1.96 and 2.23 μmol/J. Most of these works are based on hourly data from sites in the northern hemisphere. Many authors in the literature work with PAR irradiance, i.e. the global irradiance between 400 and 700 nm expressed in W/m^2, either for convenience or for operation reasons (such as indirect measurements). However, PAR irradiance and Q_p are not strictly proportional, since their ratio depends on the detailed surface solar spectrum at the time and conditions of the measurement. Frequently, this fact is ignored and an approximate conversion constant is calculated from the average incident extraterrestrial solar spectrum. This simple calculation, using the standard ASTM E490 solar spectrum (https://www.astm.org/Standards/E490.htm) normalized to a total solar irradiance of 1361 W/m^2 (Kopp and Lean, 2011) leads to a conversion constant κ=4.55 µmol/J. This value has been used in this work to convert PAR irradiance to photon flux units with the exception of the work of Tiba and Leal (2007), since these authors explicitly convert the measured photon flux to PAR irradiance using a constant of 4.60 µmol/J.

The focus of this work is the Pampa Húmeda region in south-eastern South America which is climatically and geographically homogeneous and includes parts of Argentina, Brazil and the territory of Uruguay. In this region, the percentage of surface area dedicated to agriculture and crop production is among the highest in the world (http://www.fao.org/). For this area, an average PAR fraction of 2.10 µmol/J has been reported in (Grossi Gallegos, 2004) using 26 days of hourly data. Most previous work on PAR fraction modelling has been done using hourly or daily data.

The PAR fraction f_p depends on the spectral distribution of solar radiation at ground level, which in turn depends on the state of the atmosphere (precipitable water and aerosol type and content are the main atmospheric factors identified in Alados et al, 1996) and on the air mass or, equivalently, on the Sun's altitude angle. Thus, the most relevant variables in modeling the PAR fraction f_p are the clearness index ($k_t = G_h/G_0 \cos(z)$, where $G_0 = S.F_n$ is the solar irradiance incident at the top of the atmosphere, TOA, being $S = 1361\ W/m^2$ the total solar irradiance (TSI) and F_n the orbital correction factor) and the solar altitude angle α, which can be calculated for each site and time with common calculations (Iqbal, 1983).

In this work, four pre-existing empirical models for PAR fraction estimation (which use these two variables as descriptors) are evaluated using a quality-controlled 4-year dataset with 1-minute time resolution from one site representative of the Pampa Húmeda region. Both the original and locally adapted versions of these models are evaluated. The simple approach of considering f_p = constant, commonly used by agronomical practitioners, is also considered as a performance baseline in this work. These models have been chosen for having been developed in a geographical proximity to the region of interest, with the exception of the model by Alados et al. (1996) which was developed using high quality data from Almeria, Spain. This is the first work evaluating PAR fraction models in Uruguay and one of the few on the subject working at the 1-minute time scale.

2. Data and methodology

The measurements used in this work include global horizontal irradiance (G_h or GHI), diffuse horizontal irradiance (G_{dh} or DHI) and Q_p, the PAR photon flux. They were registered between 2016 and 2019 at 1-minute intervals (average of four samples) at the experimental facility of the Solar Energy Laboratory (LES, http://les.edu.uy/) in Salto, Uruguay (latitude = -31.28°, longitude = -57.92° and altitude = 46 m above mean sea level).

Table 1: Details for the PAR fraction models evaluated in this work. The "type" column refers to whether the PAR photon flux was measured (direct) or estimated from filtered global irradiance measurements (indirect). GG is included as a previous report of the average PAR fraction (constant) for the area of interest. All models considered have been originally developed for the hourly time scale.

Label	Reference	time of measurements	length	type	Location
AL	Alados et al., 1996	1990-1992	2.5 years	direct	Almeria, Spain
TL	Tiba and Leal, 2004	2003-2004	1 year	direct	Recife, Brazil
ES	Escobedo et al., 2006	2001-2005	4 years	indirect	São Paulo, Brazil
TW	Tsubo and Walker, 2007	2000	86 days	direct	South Africa
GG	Grossi et al., 2004	2003	26 days	indirect	San Miguel, Argentina

The G_h and G_{dh} measurements were made with Kipp & Zonen CMP10 pyranometers (spectrally-flat Class A according to the ISO 9060:2018 standard). These pyranometers were mounted on a SOLYS2 Kipp & Zonen solar tracker equipped with CVF4 ventilation and heating units to prevent the accumulation of dust and water droplets on its domes. The SOLYS2 tracker was fitted with a standard shading ball assembly in order to measure G_{dh}, which in this work has been used to strengthen the quality control tests. Both pyranometers have been calibrated every two years against a Kipp & Zonen CMP22 (used as a Secondary Standard pyranometer, Abal et al., 2018) which is kept traceable to the World Radiometric Reference in Davos, Switzerland. The Q_p measurements were made using a Kipp & Zonen PQS1 quantum sensor with factory calibration at the start of the series.

2.1 Data quality

Quality control of the raw data is of the highest importance when evaluating radiation models. Our quality control procedures are applied in two steps. First, a careful inspection of the dataset is done to remove obvious anomalies (shadows, extreme values, astronomical events such as eclipses, etc.) and diurnal records are selected using the condition $cos(z) > 0$. As a result of this first process, there is a base set of 832108 positive daytime records with the three measurements used here (GHI, DHI, Q_p).

The second step consists of a set of eight quality filters (F1 to F8 in Table 1) which are applied independently to the dataset. These include the relevant BSRN quality procedures (Long and Shi, 2006) for GHI and DHI and also some restrictions on valid Q_p values, as explained below.

F1 selects records with solar altitude > 7° in order to avoid the large uncertainties typical of low-sun conditions. F2 and F3 apply BSRN upper limits with local parameters adequate for the measuring site to GHI and DHI, respectively. F4 filters out points with low clearness index k_t (associated with cloudy conditions) and low diffuse fraction f_d (clear-sky conditions).

F5 applies BSRN upper limits to f_d with a tolerance of 5 or 10 % depending on solar altitude. F6 applies an upper limit to the modified clearness index (Perez et al, 1990). F7 applies minimum and maximum limits to the PAR fraction f_p in µmol/J, obtained after inspection of the data.

Table 1: Set of quality control filters applied to the dataset and percentage discarded with respect to the base dataset of 832108 daytime records. The total solar irradiance at TOA is S = 1361 W/m^2.

Filter	Description	Condition	parameters	% discarded
F1	min solar altitude	$cos(z) > cz\,min$	cz min = 0.1219	0.7
F2	upper limit in GHI	$G_h < S.f cos^a(z) + c$	f = 1.15, a = 1.25, c = 20	0.1
F3	upper limit in DHI	$G_{dh} < S.f cos^a(z) + c$	f = 1.15, a = 1.25, c = 20	0.0
F4	lower limit for f_d	if k_t < kt max, f_d > fd min	kt max= 0.20, fd min = 0.90	2.7
F5	upper limit for f_d	for z < 75^o , f_d < fd max1 for z ≥ 75^o , f_d < fd max2	fd max1 = 1.05 fd max2 = 1.10	0.8
F6	limits on k_{tp}	0 < k_{tp} < ktp max	ktp max = 1.35	0.0
F7	limits on f_p	fp min < f_p < fp max	fp min = 1.7 *µmol/J* fp max = 10 *µmol/J*	0.4
F8	limits on Q_p	$\alpha_{min} k_t < Q_p < \alpha_{max} k_t$	α_{min} = *340 µmol/m^{2}s* α_{max} = *4000 µmol/m^{2}s*	1.5
ALL	all filters	all the above conditions		4.9

It has been observed (Foyo et al., 2017) that PAR flux data Q_p can be bounded by two straight lines in a Q_p vs k_t diagram. This can be understood since the PAR photon flux is highly correlated with global horizontal irradiance GHI, as shown in Fig. 1. If a linear relationship is assumed, $Q_p = a \times GHI = \alpha \times k_t$, with slope of $\alpha = a \times S_0 F_n / m$ expressed in terms of the relative air mass $m = 1/cos(z)$. The extreme values for this slope are associated to the extreme values of air mass in the data (between 1 and 8.21), to the 3% variation of the orbital factor (between 0.97 and 1.03) and to the natural dispersion in the (Q_p, *GHI)* diagram (Fig. 1, left) as can be understood from a simple argument. The slope, obtained by simple regression through the origin, is $a = 2.1 \pm 0.2$ µmol/J. Taking into account these variations, extreme values of α can be estimated as $\alpha_{min} \approx 340$ µmol/m^{2}s and $\alpha_{max} \approx 2900$ µmol/m^{2}s. The lower limit follows this slope quite well but the upper limit (associated to mostly clear-sky samples) does not appear to be linear in k_t, so its utilization will result in several correct samples being filtered. Therefore, filter F8 is relaxed, and thus restricts valid Q_p data to lie between two lines through the origin with slopes $\alpha_{min} = 340$

μmol/m^2s and α_{max} = 4000 μmol/m^2s, where the upper slope was increased in order to preserve valid data points for low k_t values (see Figure 1).

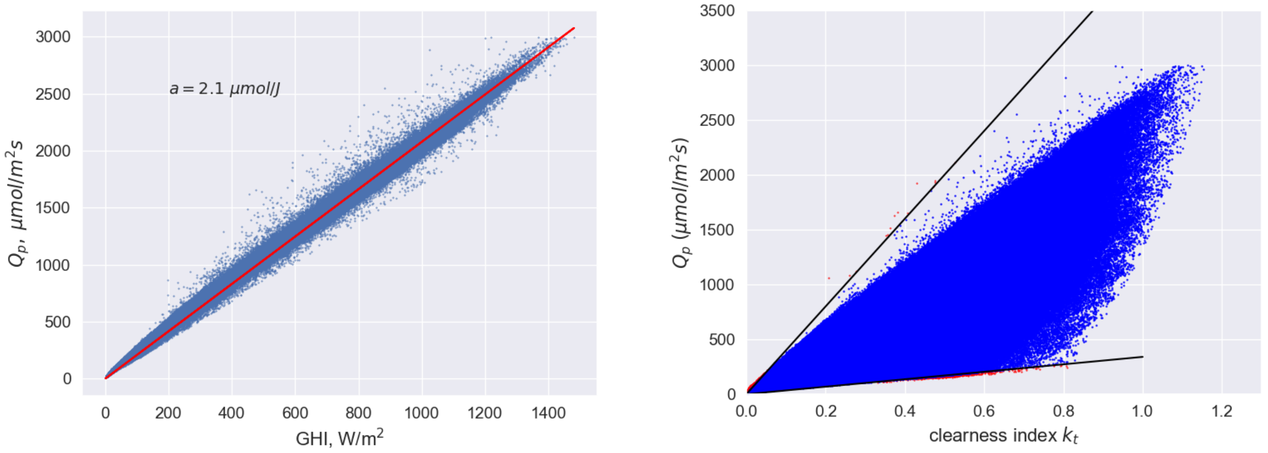

Figure 1: Left: Correlation between Qp and GHI; the red line results from a linear regression through (0,0). Right: Effect of filter F8 in the Q_p-k_t space. Discarded points appear in red. Only data that pass filters F1 to F7 are shown.

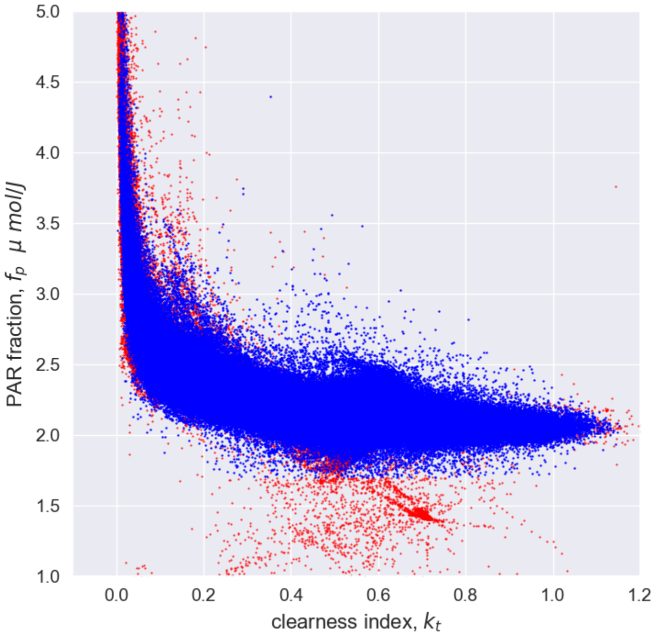

Figure 2: PAR fraction vs clearness index after all filters in Table 1 have been applied. The discarded data points are shown in red.

As shown in Table 1, less than 5% of the baseline records are discarded by this procedure, resulting in 791161 records with valid (Gh, Qp) pairs. The resulting PAR fraction vs clearness index is shown in Fig. 2.

Under heavy cloud cover (kt < 0.20) the par fraction increases sharply due to the enhanced infrared absorption associated with the predominance of diffuse irradiance (Iqbal, 1983). On the other hand, for $k_t > 0.20$, $f_p \approx 2$ μmol/J with no clear dependence on k_t.

2.2 Models and methodology

As mentioned in the introduction, the pre-existing PAR fraction models considered in this work are those listed in Table 1. All these models are based on hourly aggregated data and use the clearness index kt and the sine of the solar altitude (or, equivalently, the cos(z)) as independent predictor variables. In Ecs. (1) to (4) below, we provide the parametric form for each of these models.

AL $$f_p = a + b\,ln\left(k_t\right) + c\,sin\,\alpha_s \qquad (1)$$

TL $$f_p = a\,(sin\,\alpha_s)^b \qquad (2)$$

ES $$f_p = a + bk_t + ck_t^2 + dk_t^3 \qquad (3)$$

TW $$f_p = a + bk_t + ck_t^2 \qquad (4)$$

where *a*, *b*, *c* and *d* are coefficients (in µmol/J) that can be adjusted to local data. The original values of these coefficients are listed in Table 3. These models are supplemented by the constant value f_p = 2.096 µmol/J found from data for the Pampa Húmeda region by Grossi-Gallegos et al. (2004). Almost all models use the clearness index k_t and two of them (AL and TW) include a dependence on the relative air mass through the solar altitude angle.

The performance of these models is evaluated with their original coefficients and when the coefficients are adjusted to the local data using a standard multivariable linear regression technique. In the case of Eq. (2), the dependence on the parameter *b* is not linear, but it can be linearized by taking the natural logarithm of both sides.

The evaluation of the original models is done against the whole filtered data set. The training and evaluation of local models is done by using a standard random sampling and cross-validation method in which, at each iteration, 50% of the data is used for adjustment and the other 50% is used for testing. After 1000 iterations, the average values are used for the local parameters and for the performance indicators.

The evaluation of the models is done by calculating the residuals, $\xi = \hat{f}_p - f_p$, between the estimated PAR fraction, $\hat{f}_p$, and the corresponding measurement f_p. The mean bias deviation (MBD), the mean absolute deviation (MAD) and the root mean squared deviation (RMSD) metrics are used for the comparison,

$$MBD = \frac{1}{N}\sum_{i=1}^{N} \xi_i, \quad MAD = \frac{1}{N}\sum_{i=1}^{N} \left|\xi_i\right| \quad \text{and} \quad \text{RMSD} = \sqrt{\frac{1}{N}\sum_{i=1}^{N} \xi_i^2}, \qquad (5)$$

expressed in relative terms as a percentage of the measured PAR fraction average of 2.191 µmol/J. The integer quantity N = 791161 is the number of valid 1-min data records, resulting from the quality control procedure described in Subsection 2.1

A comparison with the original performance of some of the models is not straightforward. In some cases, these metrics are not reported. In others, it is unclear if an independent data set is used for evaluation and training. For the AL and TW PAR fraction models, independent datasets for training and evaluation are used and the absolute MBD and RMSD indicators for the derived PAR irradiance (in W/m^2) are reported, but the corresponding mean PAR irradiance is not given. In order to compare, in these cases we compute the horizontal PAR irradiance as $G_p = \kappa \times f_p \times G_h$ with κ = 4.55 µmol/J and, after expressing our relative indicators for f_p in absolute terms, obtain the desired indicators for the derived quantity, G_p.

3. Results and discussion

The previously presented models were proposed and adjusted by their authors for the hourly time scale, so they are not expected to perform as well with 1-minute data, which has significantly higher variability. This kind of comparison has been done before with diffuse fraction models (Engerer, 2015; Gueymard and Ruiz-Arias, 2016), investigating at which extent hourly models still hold or underperform when 1-min data is used. The result, of course, depends on the model.

Table 3 lists the original and locally adjusted coefficients for each model. The adjustments and performance of the original models is not only affected by the time scale of the data, but also by the typical local climate of the site and the characteristics of the data being used, so the original vs local parameter comparison is not straightforward. As a sanity check, it is noted that the sign of the parameters do not vary when locally adjusted and changes in their value are small, with the exception of the higher order terms of the ES model and the term associated with the solar altitude of the AL model.

Table 3: Original and adjusted coefficients for the PAR fraction models.

Model	Parameters	a (µmol/J)	b (µmol/J)	c (µmol/J)	d (µmol/J)
AL	original	1.83	-0.19	0.10	--
AL	locally adjusted	2.01	-0.26	-0.03	--
TL	original	1.99	-0.07	--	--
TL	locally adjusted	2.13	-0.04	--	--
ES	original	2.73	-2.39	3.46	-1.56
ES	locally adjusted	3.04	-4.83	8.29	-4.70
TW	original	2.82	-1.54	0.56	--
TW	locally adjusted	2.79	-2.07	1.48	--
constant	Grossi et al. 2004	2.10	--	--	--
constant	locally adjusted	2.19	--	--	--

Table 4 presents the performance evaluation of the models with their original coefficients, including as a baseline the constant value f_p = 0.4604 × 4.55 = 2.10 µmol/J (last row), obtained by Grossi Gallegos et al. (2004) for San Miguel, Argentina, a site located about 370 km from the LES site used for this work. The local version is the average PAR fraction obtained from our filtered dataset. They differ in about 4%, which is similar to the uncertainty in the data. The relevant performance metrics for each model (both original and locally adjusted) are given in Table 4. As expected, the constant models are the worst in terms of RMSD.

When the original models are considered, all of them fall in a narrow range: relative MBDs between 4 and 7 % and RMSDs between 8 and 11%. The hourly-adjusted polynomial models TW and ES (Tsubo and Walker, 2007; Escobedo et al., 2006) with their original coefficients provide the best local performance for 1-minute data, showing the lowest bias and dispersion. The second order polynomial of Tsubo and Walker performs slightly better, probably due to a higher robustness (polynomial instability increases with its order, specially for extrapolations). The Alados et al. model comes third in performance, quite close to the first two in terms of rRMSD, but with higher bias (indeed, the worst bias). The Tiba and Leal model with original coefficients does not improve on the utilization of a constant value for the PAR fraction, nor in bias or dispersion. The polynomial models of Eqs. (3) and (4) with their original coefficients are the ones which better represent the local data and, therefore, are the recommended original models for the region.

Table 4: Performance evaluation of the original models. The average for the relative metrics is 2.191 µmol/J.

Model	Parameters	rMBD (%)	rMAD (%)	rRMSD (%)
AL	original	-6.9	7.0	9.2
AL	locally adjusted	0.0	3.3	5.4
TL	original	-5.3	6.5	11.5
TL	locally adjusted	-0.2	6.1	10.2
ES	original	3.8	6.0	8.0
ES	locally adjusted	0.0	3.3	5.6
TW	original	-0.8	6.0	7.9
TW	locally adjusted	0.0	3.8	6.3
constant	original	-3.3	6.0	10.9
constant	local	0.0	6.5	10.4

Table 4 also presents the performance of the models with local adjustment. When the models are locally fitted, the analysis changes. The range of RMSDs is now between 5 to 10%, with negligible biases and all local models outperform the local constant value, as expected (they include extra variables with some predictive power). However, it observed that the Tiba and Leal model only improves the constant value to a small extent, hence the solar altitude as the single input variable seems to be inadequate for this problem. The models that use k_t as input show the higher improvements with respect to the local constant value. The locally adjusted model AL based on $\log(k_t)$ is the best local model, followed by the polynomial k_t models ES and TW.

Figure 3 shows the dataset for PAR fraction vs kt with the estimates from the original (violet) and the locally adjusted (red) models superposed. The PAR fraction at a 1 minute rate has an important enhancement for lower k_t values (cloudy conditions) and some locally adjusted models are not able to capture this feature in spite of their good performance metrics.

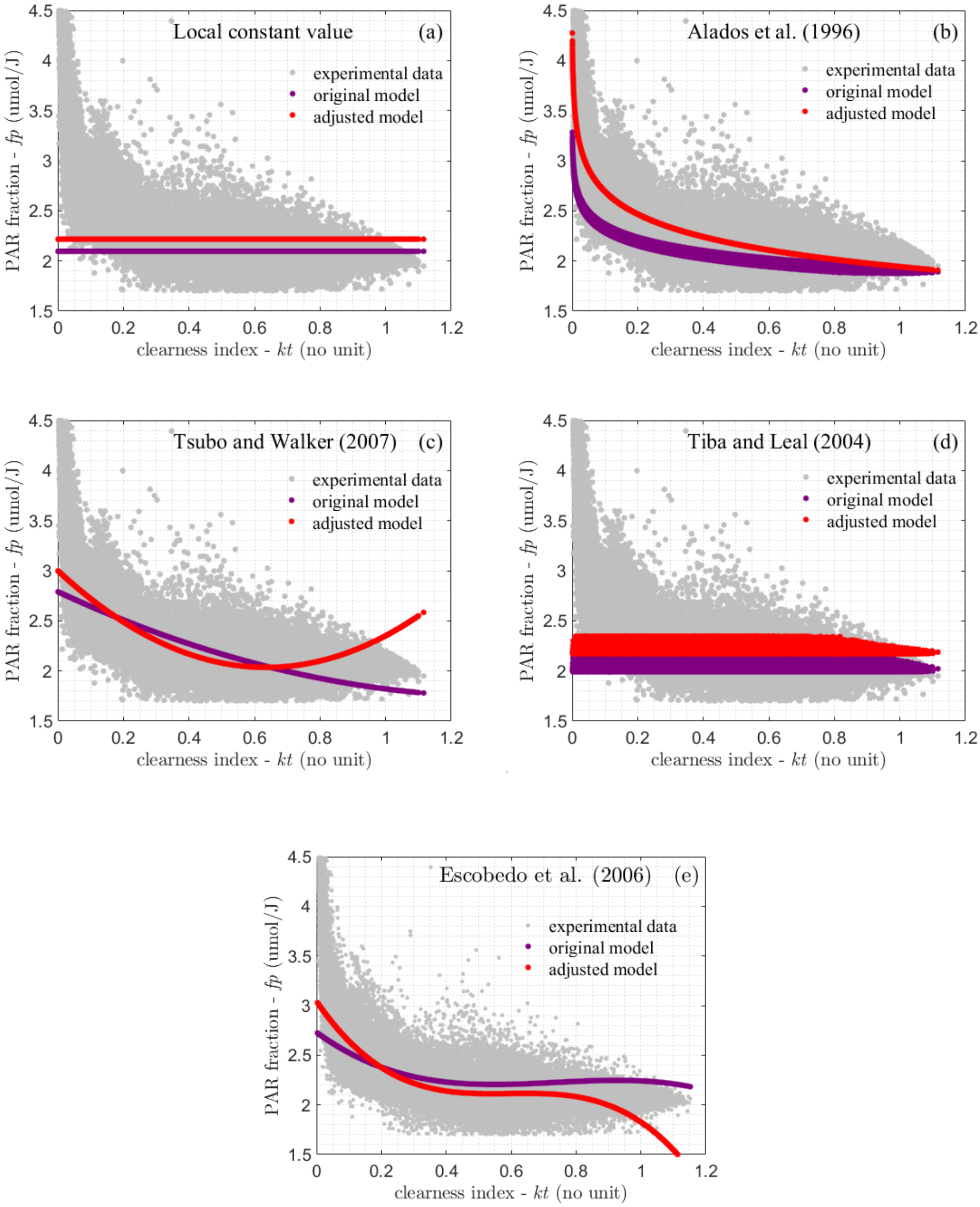

Figure 3: PAR fraction as a function of kt (1-minute time basis). Filtered data is shown as gray dots. The original model predictions are in red and the local adjusted model's predictions are shown in violet.

As Fig. 1c and 1e show (TW and ES models), the locally adjusted polynomial models are unable to adequately represent the variability of the 1-minute PAR fraction data, having acceptable overall metrics at the cost of misrepresenting data for either low or high k_t values. In particular, important deviations are observed for high k_t values (clear sky) in both polynomial models. On the other hand, the locally-adjusted AL model (Fig. 1b) adequately represents the PAR fraction tendency over the whole range of k_t. Finally, it is also observed that the constant value and the TL model are not able to reproduce the PAR fraction enhancement under cloudy skies, and this fact explains their poor performance indicators.

4. Conclusions

A first assessment of PAR fraction models in Uruguay has been presented. Four pre-existing empirical models, developed originally for the hourly timescale, were implemented and evaluated, in their original and locally adapted versions using a 1-minute quality-controlled dataset with four years of PAR flux and GHI data for a single location, representative of the Pampa Húmeda region of south-east South America. The frequently used constant model for PAR fraction has also been tested, as a baseline model. The conclusions of this work are summarized as follows:

- The average PAR fraction f_p was found to be 2.19 μmol/J, which is only 4% above the previous value for this region, obtained from indirect pyranometer-based measurements (Grossi-Gallegos et al. 2004).

- The hourly adjusted polynomial models of Escobedo et al. (2006) and Tsubo and Walker (2005) with their original coefficients represent reasonably well the local 1-minute PAR fraction data with mean biases which are -1% to 4% of mean f_p.

- Overall metrics are improved significantly by the local adaptation. In spite of this, for the TW and ES models, the local adjustment with 1-minute data is not able to represent the PAR fraction behavior for the whole range of clearness index. For this reason, their use in the region is not recommended at the 1 minute timescale. We tested higher degree polynomials (up to eight degree) and none of them was able to adequately represent the 1-minute PAR fraction behavior.

- The solar altitude as input variable provides marginal gains. The TL model, which uses only this variable, has no significant advantage over the constant model for 1-minute PAR fraction data.

- The best locally adjusted model was the one proposed in Alados et al. (1996). This model has a logarithmic dependence on the clearness index which adequately represents the 1-minute f_p behavior, especially its enhancement under overcast conditions. This was the best performing local model at the 1-minute time scale with RMSD of around 5% and negligible bias.

5. Referencias

Abal, G., Aicardi, D., Alonso Suárez, R., Laguarda, A., 2017. Performance of empirical models for diffuse fraction in Uruguay. Solar Energy, 141, 166-181.

Abal, G., Monetta, A., Alonso-Suárez, R., 2018. Outdoor solar radiometer calibration under ISO 9847:1992 standard and alternative methods. IEEE 9th Power, Instrumentation and Measurement Meeting (EPIM), pp. 1-6.

Alados, I., Foyo-Moreno, I., Alados-Arboledas, L., 1996. Photosynthetically active radiation:

measurements and modelling. Agricultural and Forest Meteorology, 78, 121-131.

Engerer, N.A., 2015. Minute resolution estimates of the diffuse fraction of global irradiance for southeastern Australia, Solar Energy, 116, 215-237. A new conventional regression model to estimate hourly photosynthetic photon flux density under all sky conditions, International Journal of Climatology https://doi.org/10.1002/joc.5063

Escobedo, J.F., Gomes, E., de Oliveira, A., Soares, J., 2006. Radiações Solares UV, PAR e IV: Estimativa em funcão da Global. ASADES, 11-79-11-86.

Foyo-Moreno, I., Alados, I. and Alados-Arboledas, L. (2017), A new conventional regression model to estimate hourly photosynthetic photon flux density under all sky

Grossi Gallegos, H., Righini, R., Dursi, O., 2004. Primeras Mediciones de la Radiación Fotosintéticamente Activa en San Miguel, Provincia de Buenos Aires. ASADES, 11.13-11.17.

Gueymard, C.A., Ruiz-Arias, J.A., 2016. Extensive worldwide validation and climate sensitivity analysis of direct irradiance predictions from 1-min global irradiance, Solar Energy, 128, 1-30.

Iqbal, M., An Introduction to Solar Radiation. Academic Press, Toronto, 1983.

Kopp, G. and Lean, J.L., A new, lower value of total solar irradiance: Evidence and climate significance, 2011. Geophysical Research Letters, 38, L01706, doi:10.1029/2010GL045777.

Long C.N. and Shi Y. 2006. The QCRad Value Added Product: Surface Radiation Measurement Quality Control Testing, Including Climatologically Configurable Limits. Atmospheric Radiation Measurement Program, Technical Report, ARM TR-074. Available at http://www.arm.gov/publications/tech_reports/doe-sc-arm-tr-074.pdf

Perez, R., Inechien, P., Seals, R. and Zelenka, A., 1990. Making full use of the clearness index for parameterizing hourly insolation conditions. Solar Energy 45, pp 111-114.

Tiba, C., Leal, S., 2004. Medidas e Modelagem da Radiação PAR para o nordeste do Brasil. 5º Encontro de Energia no Meio Rural e Geração Distribuída, pps. 1-8, Campinas, São Paulo.

Tsubo, M., Walker. S., 2005. Relationships between photosynthetically active radiation and clearness index at Bloemfontein, South Africa. Theor. Appl. Climatol., 80, 17-25.